

Identifying man-made objects along urban road corridors from mobile LiDAR data

Hongchao Fan¹ and Wei Yao²

¹Chair of GIScience, Heidelberg University, Berlinerstr. 48, 69120 Heidelberg, Hongchao.fan@geog.uni-heidelberg.de

²Department of Photogrammetry, the Technical University of Munich, Arcisstr.21, 80333 Munich, Germany, wei.yao@bv.tum.de

Abstract—

This letter is dedicated to an automated approach for the detection and classification of man-made objects in urban corridors from point clouds acquired by vehicle-borne Mobile Laser Scanning (MLS). The approach is designed based on a-priori knowledge in urban areas: (i) man-made objects feature geometric regularity like vertical planar structures (e.g. building facades), while vegetation reveals a huge diversity in shape and point distribution; (ii) different types of urban man-made objects can be characterized by the point extension and height above the ground. Therefore, MLS-based point clouds are first divided into three layers with respect to the vertical height dimension. In each layer, seed points of man-made objects are indicated by a line-filter in the footprints of off-ground objects which is generated by binarizing the spatial accumulation map of point clouds. These seed points are further classified by examining in which layers the seed points of objects are found. Finally, points belonging to respective objects can be retrieved based on classified seed points. The experiments show that various man-made objects on both street sides can be well detected with a detection rate of up to 83%. For the classification of detected urban objects, an overall accuracy of 92.37% can be achieved.

Index Terms— Mobile laser scanning, detection, classification, man-made objects, spatial accumulation

I. INTRODUCTION

As the need for detailed and accurate 3D information about urban objects continues to increase, automatic object extraction, classification and reconstruction in urban areas are active research topics in the field of LiDAR remote sensing. The extracted and reconstructed models for urban objects, such as building, road, vehicle, tree, pole and traffic sign, constitute an invaluable data source for map updating, 3D city modeling and driver navigation applications. Many efforts have been made to address this problem by integrating multi-sources remotely sensed data including optical images and LiDAR data.

Recently, airborne LiDAR data have been widely used to extract buildings, vehicles and vegetation. The methods for extracting urban objects from airborne LiDAR data usually consist of three steps: geometric filtering, feature calculation and classification [1,2]. Some of methods include an object-based point cloud analysis strategy for extraction of vegetation and vehicles [2,3]. Unlike the airborne LiDAR data, vehicle-borne mobile LiDAR data acquire object information from a ground perspective and provide much more detailed information about scanned objects along road corridors[4-6]. It leads to a great potential for object extraction at the street level and high-fidelity reconstruction of object models. To classify and extract various objects from mobile LiDAR data, basic geometric structures

such as plane, vertical pole and volumetric cluster are firstly extracted to represent the primitives for urban objects. [7-11] presented approaches for automatic extraction of vertical walls, vegetation, road markings and poles, respectively. These works require a model-based approach to deal with the extraction of specific object classes which is often limited to object knowledge at local level. Since MLS data feature the high object fidelity and huge data volume could affect the efficiency of automation of the processing, approaches for the detection and fine classification of above-ground objects along urban roads are still needed. However, most of former works [7-11] focused on extracting single object classes by designing class-specific features and adopting model-based approaches. Such approaches could be complex to be combined for processing urban area with many different types of objects.

This letter proposes an automated approach for the detection and classification of man-made objects from MLS-based point clouds of urban corridors. The approach consists of four stages (Fig.1): (i) the pre-processing step; (ii) the stage for extracting seed points of man-made objects; (iii) the stage of distinguishing seed points into different types of man-made objects; and (iv) the stage of identifying 3D points of the man-made objects.

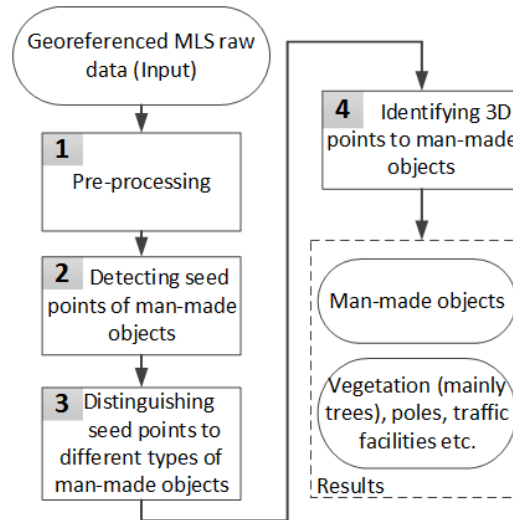


Fig.1 Workflow diagram for the proposed approach

The remainder of this letter is organized as follows: Section II briefly describes the pre-processing. Section III presents the method of finding seed points of man-made objects. Section IV describes the method of distinguishing seed points into different types of man-made objects. In Section V, a mechanism is introduced to identify 3D points of individual man-made objects based on the extracted seed points. Section VI demonstrates the experiments and discusses results. Section VII concludes the whole work.

II. PRE-PROCESSING

In this stage, ground points are detected by analyzing the height histogram [12] and are further delivered to a surface fitting algorithm (Gridfit) [13] to obtain a raster representing ground surface. The vertical distance of each point to the ground level is calculated as the height Above the Ground Level (AGL). In general, off-ground objects can be divided into two classes: man-made objects and nature objects. Man-made objects are normally referred to a large variety of buildings, power lines and poles, cars, and other city facilities, while nature objects are mainly referred to vegetation.

With respect to the AGL height, man-made objects are characterized as follows: (i) fences or vehicles are lower than two meters; (ii) buildings are higher than two meters above the ground; and (iii) power lines hanging in the air and having the minimum AGL height of five meters. In MLS data, the former

two kinds of objects are represented mainly by vertical structure points; while the latter has great elongation in the horizontal dimension. In contrast, vegetation reveals huge diversity in the spatial point distribution. Additionally, a vehicle might be parked under a tree; part of a tree grows over the fence or building's roof. In such cases, it can lead to detection errors when using the method of projecting 3D points onto one single horizontal accumulator as presented in [14-15]. In order to reduce extraction errors and to enhance the individualization level of the aforementioned objects, off-ground MLS-based point clouds are divided here into three layers according to AGL height (see Fig.2).

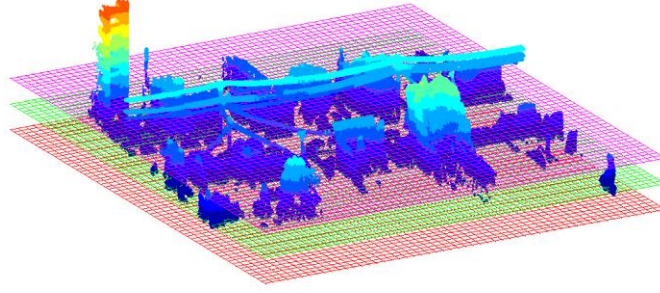


Fig.2 Projecting point clouds layerwise onto horizontal grid-cell accumulator

III. DETECTING SEED POINTS FOR MAN-MADE OBJECTS

The second stage aims to extracting seed points of man-made objects. It is proposed based on several assumptions. Firstly, man-made objects have regular geometric features like vertical planar structures (for instance facades of buildings), while vegetation reveals a huge diversity in shapes. If the 3D points are projected onto the horizontal plane, there will be high accumulation density wherever man-made objects are located. Secondly, in the lower layer different types of off-ground objects are situated very closely, but with a minimum distance of half meters. Thirdly, power lines are isolated by other urban objects.

According to the first assumption, for the three layers, an accumulation space of a 2D $M \times N$ grid (Fig.2.) using the similar method to [14] is created on the horizontal plane respectively, whereby $M = \text{ceil}((X_{\max} - X_{\min})/S_x)$, and $N = \text{ceil}((Y_{\max} - Y_{\min})/S_y)$. The size of cell (S_x, S_y) depends on the density of laser points on vertical plane i.e. facades. Normally, it should be set so small, so that the detail of footprint geometry will be well preserved. Then it counts how many points fall within each cell. Setting a threshold N_T for the accumulation space, if the accumulation density within a cell is more than the threshold $(N_p \geq N_T)$ ¹, the middle point of these points is calculated and kept for the cell. Otherwise, the cell is kept as empty.

$$G_{foot} = \begin{cases} \emptyset, & N_p < N_T \\ X_{foot} = \frac{1}{N_p} \sum_{i=1}^{N_p} X_i, Y_{foot} = \frac{1}{N_p} \sum_{i=1}^{N_p} Y_i, & N_p \geq N_T \end{cases} \quad (1)$$

where, $G_{foot}(X, Y)$ stands for the middle points of those points (X_i, Y_i) falling in a cell, and N_p is the number of points falling within the cell.

The points resulted by Eq.1 form a map of footprints. As shown in Fig. 3a, the map contains not only the footprints of man-made objects, but also footprints of vegetation. In many cases, there are noise measurements too. For extracting seed points of man-made objects, the points on the footprint map are

¹ On the accumulators of lower layer and middle layer, the threshold N_{T1} should be so set as a significantly large number, since structures such as facades, fences, poles, and trucks of trees are scanned with high dense laser points in the vertical dimension. In the contrast, the threshold N_{T2} for upper layer should be set as a smaller number because horizontal structures are recorded with low density of laser points. According to experiences in our experiments, the threshold is set as 30 in the data processing (Section VI).

first clustered by checking the point-to-point connectivity, whereby the maximum distance of a point to its nearest neighbor in a cluster should be smaller than 0.5m which means the minimum point-pair distance between two clusters should be larger than 0.5m. As the results (Fig.3b), points are clustered to footprints of an object when they are located closely to each other. In other words, each cluster contains footprints of individual objects above the ground. Man-made objects differ from vegetation and noise measurements in the fact that they show linear structures in the footprint map. Aiming to extract such linear structures, the map of footprints is converted into a binary image (Fig.3c) by taking grid cell as pixel, where the pixel value is set as 1 for a non-empty cell and 0 for an empty cell. Then, edges are detected using Canny operator with sensitivity thresholds of [0.1 0.2] and the sigma of the Gaussian filter is set to 1. The extracted linear edges (Fig.3d) are aggregated to a long line segment if they are collinear and adjacent. In the next step, remaining edges are filtered by setting a length threshold. In this work, the length threshold is set to two meters, as it should be shorter than the minimum edge of a building footprint. On the other hand, a car is normally longer than two meters. As the result (Fig.3e) only line segments of building footprints, fences and vehicles remain.

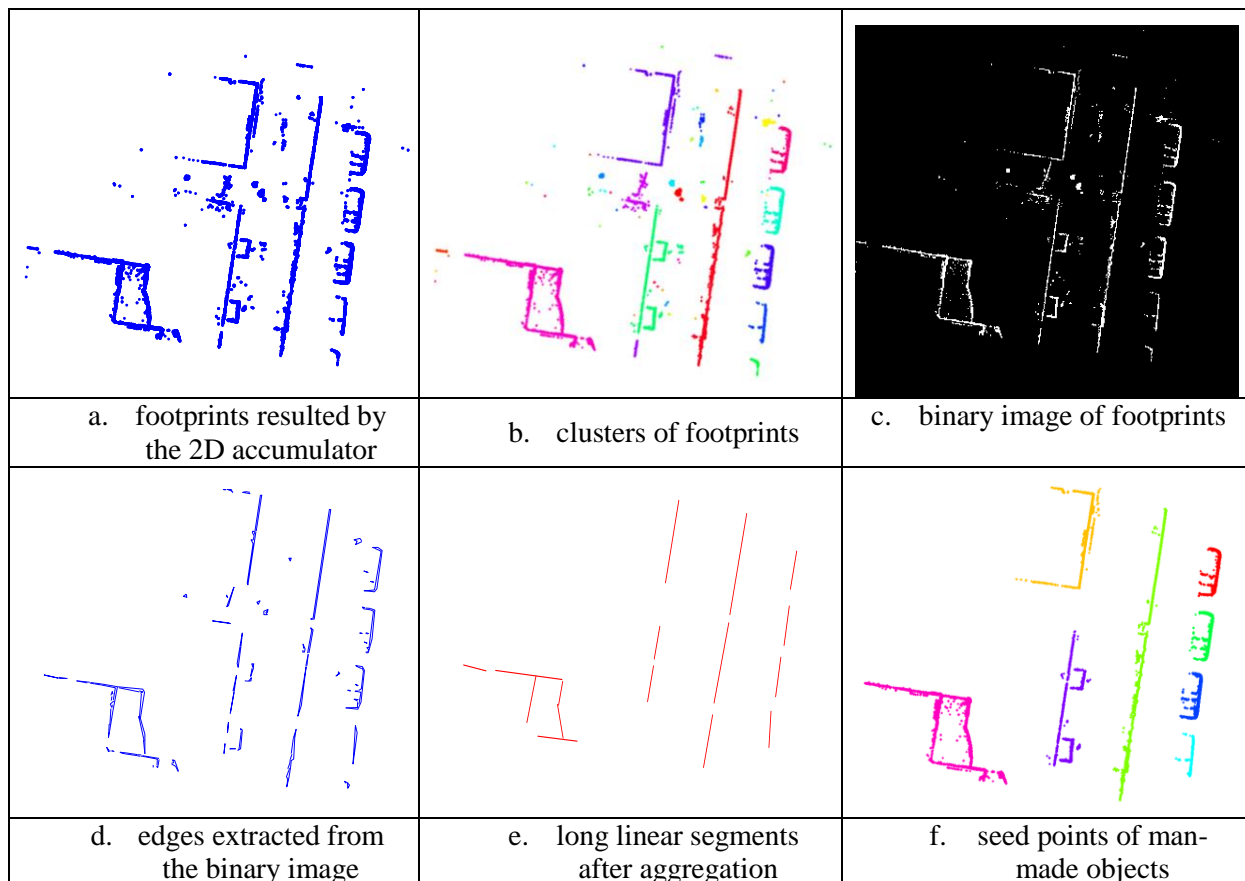


Fig.3 Extraction of line segments from footprints

When transferring extracted line segments back to the domain of the footprint map, the clusters should correspond to footprints of man-made objects, if they are located on or close to a line segment. Fig.3f shows the seed points of man-made objects, where seed points of individual objects are visualized in different colors.

In the presented approach, a matching process is conducted by checking if a cluster is overlapped by the buffer zone of extracted line segments. A buffer zone is a rectangle (see Fig.4) which is generated around a line segment by setting the long axis parallel to line segment and a width of one meter ($d = 0.5m$) considering the accuracy of edge extraction and transformation. Points which are located

within the buffer zones should be seed points of man-made objects. The rectangle is generated as a buffer zone P_b for the line segment according to Eq.2.

$$P_{b,i} = P_m + P_i \cdot \begin{pmatrix} \cos(\theta) & \sin(\theta) \\ -\sin(\theta) & \cos(\theta) \end{pmatrix}, i = 1,2,3,4 \quad (2)$$

where $P_{i=1,2,3,4} = \left[\left(\frac{s}{2} + d, -d \right) \left(\frac{s}{2} + d, d \right) \left(-\frac{s}{2} - d, d \right) \left(-\frac{s}{2} - d, -d \right) \right]$, P_m is the middle point of the line segment $\overline{P_a, P_e}$, s is the length of the line segment, and θ is the orientation of the line segment.

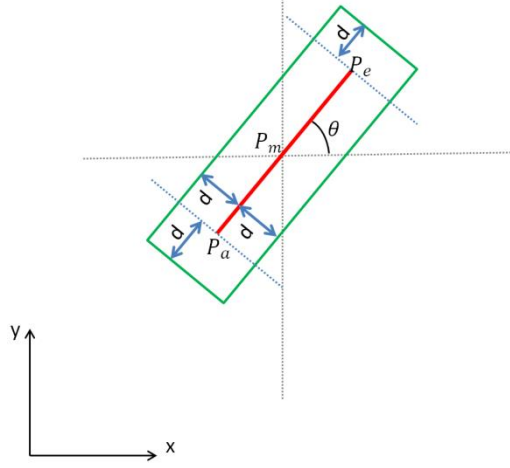


Fig. 4 Buffer zone for a line segment on footprint-map

IV. DISTINGUISHING SEED POINTS FOR MAN-MADE OBJECTS

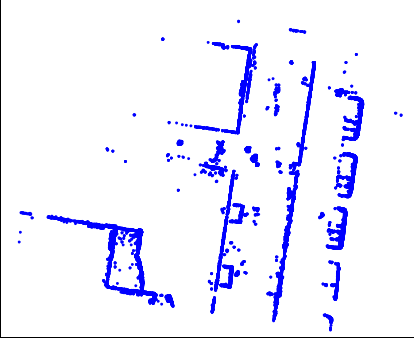
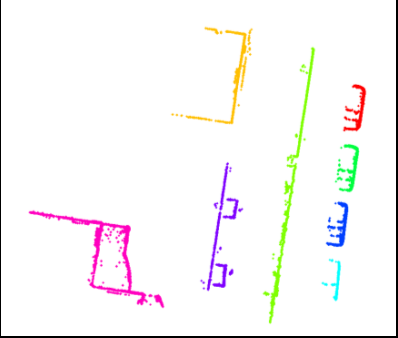
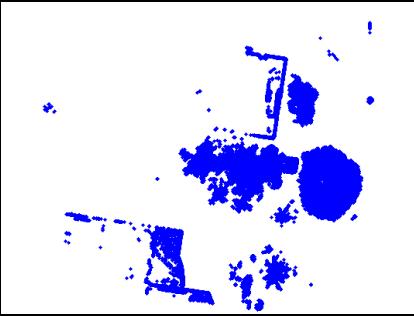
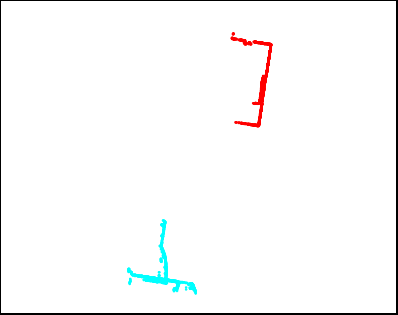
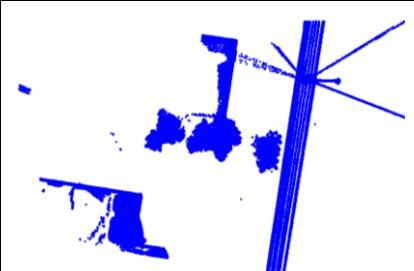
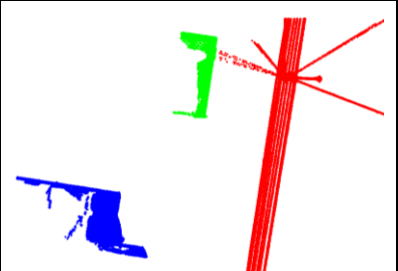
The results of the last step are seed points of man-made objects in three layers. They clustered as every cluster corresponds to an individual object, which will be distinguished into different types of objects in this Section. As discussed in Section II, cars and fences only exist in the lower layer ($h \leq 2m$), while power lines can only be found in the upper layer ($h \geq 5m$), and points of buildings could be found in every layer. According to this, the seed points can be distinguished by performing the cross-comparison through layers.

- For a cluster G_{lower} in the lower layer, if there is a cluster G_{middle} in the same location on the middle layer, the points in the cluster G_{lower} are seed points of a building. Otherwise, the points of cluster G_{lower} are seed points of a car or a piece of fence.
- For a cluster G_{upper} in the upper layer, if there is no cluster in the same location on the middle layer, the points in the cluster G_{upper} are seed points of power lines.
- Seed points of cars and fences can be distinguished by length, where the length of a cluster of seed points is calculated as the maximal distance between the seed points. According to the empirical knowledge, a car is normally shorter than 6 meters.

In this letter, point pairs are found out between two clusters (e.g. $G_{lower,a}(P_{i=1,\dots,M})$, $G_{middle,b}(P_{j=1,\dots,N})$) on different layers. Whereby, two points (P_i, P_j) can be paired if they are almost identical $d(P_i, P_j) \leq 0.05m$ on 2D plane (their distance is smaller than 5cm, $d(P_i, P_j) \leq 0.05m$). If most of points in a cluster on a layer can be paired to points in a cluster on the other layer $\frac{K}{\min(M,N)} \geq 95\%$, these two cluster are assumed to be in the same location, where K stands for the number of the paired points.

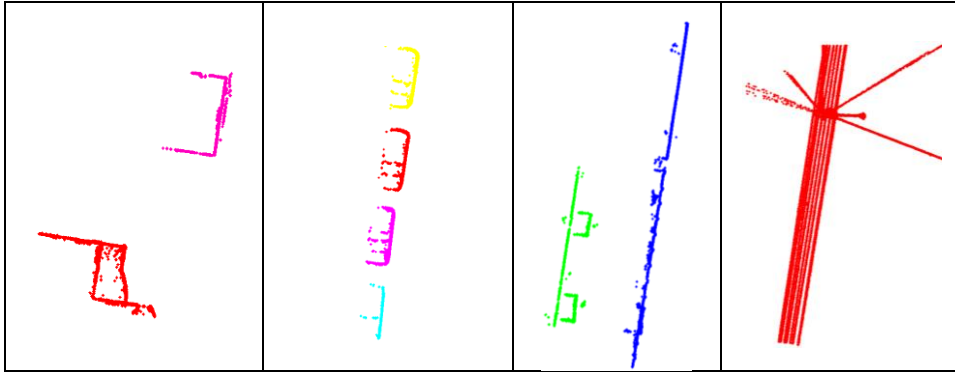
Tab.1 shows examples of results of seed points extracted from three layers. In general, there are only footprints of man-made objects on the map of seed points, whereas there are also noises and footprints of other types of objects on the original map of footprints. Totally, eight man-made objects are detected from the footprints of the lower layer, while two objects are detected from the middle layer. And three man-made objects are detected in the upper layer. After comparing detected clusters in terms of their locations through the three layers, two buildings are detected, because their seed points exist both in lower and middle layers. Four cars and two pieces of fences are detected, since their seed points can only be found in the lower layer. One object of power lines is detected, because its seed points can only be verified in the upper layer. It should be pointed out that footprints of trees and the noise measurements cannot affect the results of extracting and distinguishing seed points of man-made objects, because no line segments can be extracted from the points of these footprints, as demonstrated in Tab.1.

Tab. 1 Distinguishing seed points into different types of urban objects

	Original map of footprints	Seed points of man-made objects in diff. layers
Lower layer		
Middel layer		
Upper Layer		

Tab. 2 Seed points of different man-made objects

Seed points of building	Seed points of cars	Seed points of fences	Seed points of power line



V. EXTRACTING MAN-MADE OBJECTS

After seed points are extracted for different man-made objects, 3D points of individual man-made objects can be identified according to the topological relation to seed points. This is achieved by a two-step approach. Firstly, the convex hull of each cluster of seed points is calculated in order to reduce the search area. The spatial relation of points falling within the convex hull of seed points is calculated. The convex hull is calculated for each cluster of seed points:

- the seed points of an object class are examined regardless of their heights. If a point is located inside of (and on) the convex hull of the cluster of seed points, this point is regarded as candidate point of object class

In the next step, a circle neighborhood with a radius of 0.5m is generated for every seed point in the cluster, considering the roughness of building facades. Then candidate points are checked if they are falling within this circle. Those points are regarded to have the same footprint as the seed point, if they fall within the circle of the seed point. And they are of course points belonging to the object corresponding to the seed cluster. Finally, all the points belonging to the object are identified. The points that do not fall in any circle of the seed point will be released from the candidate points, as they do not belong to the object. Tab.3 shows the 3D points of the extracted man-made objects of different types (compared with Tab.1&2).

Tab.3 Extracted points of various man-made objects

buildings	Cars	fences	power line

VI. EXPERIMENTAL RESULTS AND DISCUSSION

The point clouds of urban road corridor used in this study were captured by an Optech Lynx Mobile Mapper system, which consists of two Optech laser scanners, one GPS receiver, and an Applanix IMU, which collects LiDAR data at more than 100,000 measurements per second with a 360° field of view. The point clouds of two sites were selected for assessing the performance of the proposed method. The two test sites are located in an urban residential area with dimensions of 190 m by 130 m. It contains vegetation (e.g., trees, bushes), fences, buildings, power lines, multi-lanes roads, and cars. Reference data for different object classes were directly selected by human inspection in LiDAR point clouds. The proposed approach is composed of two sequential steps: detection and classification of man-made

objects. Since the classification is conducted along with the object detection, its results are also evaluated based on those of detection. To this end, both evaluations of detecting and classifying man-made objects are shown in Tab.4 and Tab.5, respectively.

Tab.4 shows the accuracy of detecting man-made objects. There are 20-30% misdetections. The results depend on how dense the man-made objects are scanned by MLS. If their vertical components are scanned with complete points, the man-made objects can be better detected. Otherwise, it is difficult or impossible to detect, if their vertical components are occluded and measured with low dense points. Fig.5 demonstrates several types of misdetection. Fig.5a, the building (within the white box) cannot be detected, because its facades are occluded by buildings in front and cannot be scanned with points of sufficient density. The power lines on this image cannot be detected, too, since they are scanned with low dense points and therefore cannot be extracted as lines on the binary image. Fig.5b shows that a number of cars cannot be detected because only their roofs are captured. Fig.5c gives an example of a piece of fence in mixture type of cyclone fence and live fencing. This kind of fence is hard to be detected because a large number of laser points fly through the spaces of the fence; hence not so many points meet the fence and lead to enough accumulation density on the accumulator.

Tab.4 Results of detection

	Building	Car	Fence (pieces)	Fence (m)	Power line (m)
Manual identification	46	65	41	385.19	683.70
Automated detected	32	46	31	297.75	568.61
Detection rate	69.57%	70.77%	75.61%	77.30%	83.17%

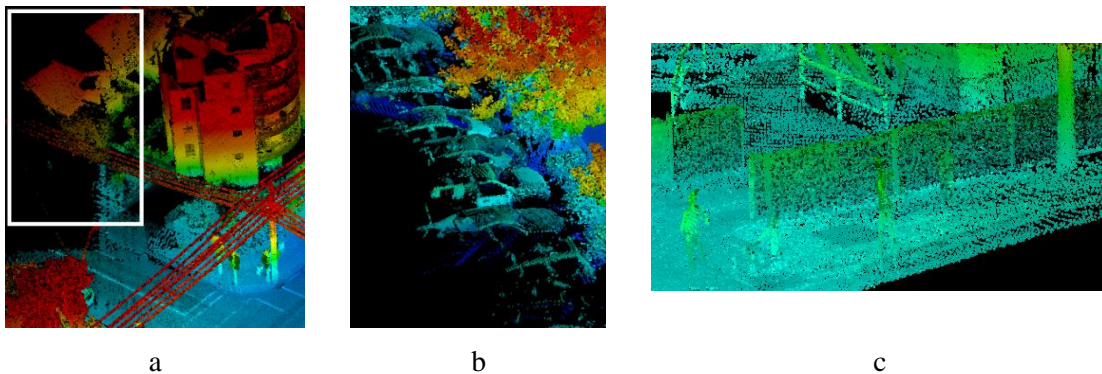


Fig.6 Examples for misdetection (color of points indicates the AGL height)

The confusion matrix in Tab.5, calculated by 3-fold cross-validation, shows the results of the classification. In our experiments, an overall accuracy of 92.37% has been achieved, where cars have been classified with the best accuracy. Only one cottage is classified as four pieces of fences, because it is not high enough to form a man-made object in the middle layer. Some pieces of short rock fences have been classified as cars, because they have similar length to cars. The assignment of threshold values depends on the average density of the measurement in data sets. They can be determined by checking several man-made objects which need to be manually detected in advance. Then these values can be used for the whole data set automatically. In other words, it needs only some efforts for

determining these values prior to the automatic process, in the case that the approach can be deployed for different data sets.

Tab.5 Results of classification

	Building	Car	Fence
detected building	32	0	0
detected car	0	46	5
detected fence	4	0	31
Producer accuracy	88.89%	100%	86.11%

VII. CONCLUSION

In this letter a novel approach has been proposed for identifying man-made objects from MLS-based point clouds of urban areas. The approach is developed based several a-priori knowledge according to which the laser points are divided into three layers. Then, seed points of man-made objects are extracted by a line-filter in the footprint map of off-ground objects. Finally, points belonging to respective objects can be retrieved based on classified seed points. The experiments show that various man-made objects on both street sides can be well detected with a detection rate of up to 83%. For the classification of detected urban objects, an overall accuracy of 92.37% can be achieved.

Although the proposed approach can extract man-made objects with high completeness and accuracy, it also has some limitations. First, trucks might be detected as small houses, because they are normally higher than two meters. Secondly, other kinds of fences e.g. cyclone fence, Ha-ha fence, picket fence, etc. are difficult to be detected. Thirdly, the power lines scanned with low density points cannot be detected. Fourthly, some isolated short fences are classified as cars. In the future, the last two shortcomings will be overcome by analyzing the 3D shapes of detected objects. At the same time, methods will be developed to distinguish lamp posts and traffic signs from vegetation.

ACKNOWLEDGMENT

REFERENCES

- [1] C. Mallet, U. Soergel, and F. Bretar, "Analysis of full waveform LiDAR data for an accurate classification of urban areas," In: International Archives of Photogrammetry, Remote Sensing and Spatial Information Sciences. Vol. 37 (Part 3A). Beijing, China, 2008.
- [2] M. Rutzinger, B. Höfle, M. Hollaus, and N. Pfeifer, "Object-based point cloud analysis of full-waveform airborne laser scanning data for urban vegetation classification," *Sensors*. Vol. 8(8), pp. 4505-4528, 2008.
- [3] W. Yao, S. Hinz, and U. Stilla, "Extraction and motion estimation of vehicles in single-pass airborne LiDAR data towards urban traffic analysis," *ISPRS Journal of Photogrammetry and Remote Sensing*, 66(3), 260-271, 2011.
- [4] A. Kukko; H. Kaartinen; J. Hyyppä; Y. Chen, "Multiplatform Mobile Laser Scanning: Usability and Performance," *Sensors*, 2012, 12, 11712-11733.
- [5] S. Pu, M. Rutzinger, G. Vosselman., S O, Elberink, "Recognizing basic structures from mobile laser scanning data for road inventory studies," *ISPRS Journal of Photogrammetry and Remote Sensing*, Volume 66, Issue 6, Pages S28-S39, Supplement, 2011.
- [6] A. Jaakkola, J. Hyyppä, A. Kukko, X. Yu, H. Kaartinen, M. Lehtomäki, and Y. Lin, "A low-cost multi-sensoral mobile mapping system and its feasibility for tree measurements," *ISPRS Journal of Photogrammetry and Remote Sensing*, Volume 65, Issue 6, Pages 514-522,2010.

- [7] K. Hammoudi, F. Dornaika, B. Soheilian, and N. Paparoditis, "Extracting wire-frame models of street facades from 3D point clouds and the corresponding cadastral map," in Proc. Int. Arch. Photogrammetry, Remote Sensing and Spatial Information Science, 2010, vol. 38, pp. 122-139.
- [8] M. Rutzinger, A. K., Pratihast, S. J, Oude Elberink and G. Vosselman, " Tree modelling from mobile laser scanning data-sets," The Photogrammetric Record, Papers 26, 361-372, 2011.
- [9] B. Yang, L. Fang, Q. Li, and J. Li, "Automated Extraction of Road Markings from Mobile Lidar Point Clouds," Photogrammetric engineering and remote sensing, vol. 78, no4, pp. 331-338, May. 2012.
- [10] R. Wang, J. Bach, and F.P, Ferrie, "Window detection from mobile LiDAR data," Applications of Computer Vision (WACV), 2011 IEEE Workshop on, vol., no., pp.58-65, 5-7 Jan. 2011.
- [11] M. Lehtomäki, A. Jaakkola , J. Hyypä, A. Kukko, H. Kaartinen, "Detection of Vertical Pole-Like Objects in a Road Environment Using Vehicle-Based Laser Scanning Data," Remote Sensing, ; 2(3):641-664, 2010.
- [12] W. Yao, S. Hinz, and U. Stilla, "Automatic Vehicle Extraction from Airborne LiDAR Data of Urban Areas aided by Geodesic Morphology," Pattern Recognition Letters, Vol.31, no.10, pp.1100-1108, 2010.
- [13] D'Errico, 2006 D'Errico, J., 2006, Surface fitting using gridfit. <http://www.mathworks.com/matlabcentral/fileexchange>(accessd on 10.01.2009)
- [14] K. Hammoudi, F. Dornaika and N. Paparoditis, "Extracting building footprints from 3D point clouds using terrestrial laser scanning at street level," In: Stilla U., Rottensteiner F., Paparoditis N. (Eds) CMRT09. IAPRS, Vol. XXXVIII, Part3/W4, Paris, France, 3-4 September, 2009.
- [15] K. Hammoudi, F. Dornaika, B. Soheilian, B. Vallet, J. McDonald and N. Paparoditis. Recovering Occlusion-Free Textured 3D Maps of Urban Facades by a Synergistic Use of Terrestrial Images, 3D Point Clouds and Area-Based Information, Procedia Engineering, Volume 41, pp. 971-980, 2012.